

THE STATUS OF VIRGO

F.ACERNESE⁶, P.AMICO¹⁰, S.AOUDIA⁷, S.AVINO⁶, D.BABUSCI⁴, G.BALLARDIN², R.BARILLÉ²,
F.BARONE⁶, L.BARSOTTI¹¹, M.BARSUGLIA⁸, F.BEAUVILLE¹, M.A.BIZOUARD⁸, C.BOCCARA⁹,
F.BONDU⁷, L.BOSI¹⁰, C.BRADASCHIA¹¹, S.BRACCINI¹¹, A.BRILLET⁷, V.BRISSE⁸, L.BROCCO¹²,
D.BUSKULIC¹, E.CALLONI⁶, E.CAMPAGNA³, F.CAVALIER⁸, R.CAVALIERI², G.CELLA¹¹, E.CHASSANDE-
MOTTIN⁷, A.-C.CLAPSON⁸, F.CLEVA⁷, J.-P.COULON⁷, E.CUOCO², V.DATTILO², M.DAVIER⁸, R.DE ROSA⁶,
L.DI FIORE⁶, A.DI VIRGILIO¹¹, B.DUJARDIN⁷, A.ELEUTERI⁶, D.ENARD², I.FERRANTE¹¹, F.FIDECARO¹¹,
I.FIORI¹¹, R.FLAMINIO^{1,2}, J.-D.FOURNIER⁷, S.FRASCA¹², F.FRASCONI^{2,11}, A.FREISE², L.GAMMAITONI¹⁰,
A.GENNAI¹¹, A.GIAZOTTO¹¹, G.GIORDANO⁴, L. GIORDANO⁶, R.GOUATY¹, D.GROSJEAN¹, G.GUIDI³,
S.HEBRI², H.HEITMANN⁷, P.HELLO⁸, L.HOLLOWAY², S.KRECKELBERGH⁸, P.LA PENNA², V.LORIETTE⁹,
M.LOUIAS², G.LOSURDO³, J.-M.MACKOWSKI⁵, E.MAJORANA¹², C.N.MAN⁷, F.MARCHESONI¹⁰,
F.MARION¹, J.MARQUE², F.MARTELLI³, A.MASSEROT¹, M.MAZZONI³, L.MILANO⁶, C.MOINS²,
J.MOREAU⁹, N.MORGADO⁵, B.MOURS¹, A.PAI¹², C.PALOMBA¹², F.PAOLETTI^{2,11}, S.PARDI⁶,
A.PASQUALETTI², R.PASSAQUIETI¹¹, D.PASSUELLO¹¹, B.PERNIOLA³, F.PIERGIOVANNI³, L.PINARD⁵,
R.POGGIANI¹¹, M.PUNTURO¹⁰, P.PUPPO¹², K.QIPIANI⁶, P.RAPAGNANI¹², V.REITA⁹, A.REMILLIEUX⁵,
F.RICCI¹², I.RICCIARDI⁶, P.RUGGI², G.RUSSO⁶, S.SOLIMENO⁶, A.SPALLICCI⁷, R.STANGA³, R.TADDEI²,
D.TOMBOLATO¹, E.TOURNEFIER¹, F.TRAVASSO¹⁰, D.VERKINDT¹, F.VETRANO³, A.VICERÉ³, J.-
Y.VINET⁷, H.VOCCA¹⁰, M.YVERT¹, Z.ZHANG²

¹Laboratoire d'Annecy-le-Vieux de physique des particules, Annecy-le-Vieux, France

²European Gravitational Observatory (EGO), Cascina (Pi) Italia

³INFN, Sezione di Firenze/Urbino, Sesto Fiorentino, and/or Università di Firenze, and/or Università di Urbino, Italia

⁴INFN, Laboratori Nazionali di Frascati, Frascati (Rm), Italia

⁵SMA, IPNL, Villeurbanne, Lyon, France

⁶INFN, sezione di Napoli and/or Università di Napoli "Federico II" Complesso Universitario di Monte S. Angelo, Napoli, Italia and/or Università di Salerno, Fisciano (Sa), Italia

⁷Département Artemis - Observatoire Côte d'Azur, BP 42209, 06304 Nice, Cedex 4, France

⁸Laboratoire de l'Accélérateur Linéaire (LAL), IN2P3/CNRS-Univ. De Paris-Sud, Orsay, France

⁹ESPCI, Paris, France

¹⁰INFN Sezione di Perugia and/or Università di Perugia, Perugia, Italia

¹¹INFN, Sezione di Pisa and/or Università di Pisa, Pisa, Italia

¹²INFN, Sezione di Roma and/or Università "La Sapienza", Roma, Italia

Presented by C. Bradaschia, INFN, Sezione di Pisa, Pisa Italia.

Virgo is a 3 km arm laser interferometer aiming at the detection of gravitational waves in a range of frequency between 5 Hz and 5 kHz. Virgo has been built in the vicinity of Pisa – Italy, by a collaboration among several laboratories of CNRS (France) and INFN (Italy). The construction has been completed in 2003. 2004 has been devoted to commissioning the detector, with the aim to start the acquisition of scientifically interesting data in 2005. The status of advancement of the commissioning will be reported and the present sensitivity will be discussed.

1 Introduction

In this paper we will describe the main characteristics of the interferometric gravitational wave detector Virgo ¹ and its status of advancement towards full scientific operation. Other gravitational wave detectors exist all over the world, at different stages of development; they are of two different types: resonant bars and laser interferometers. For the general features of gravitational waves, astrophysical sources and detectors, the reader is invited to refer to the paper presented to this conference by D. Blair ².

It is worth to remark that a laser interferometer “à la Michelson” is extremely sensitive to changes of the arm length difference. Hence an interferometer seems to be the ideal instrument to detect the passage of gravitational waves, whose effect is to alternatively stretch and squeeze

distances between free falling masses, in two orthogonal directions of the wave-front plane. In an interferometric detector, the mirrors limiting the arms, suspended to pendulum chains, can be considered “free falling masses”, virtually free in the horizontal interferometer plane.

High sensitivity is required by the extremely small arm length change ($\Delta L = h L = 10^{-21} L$; hence ΔL is of the order of 10^{-18} m for kilometric arm interferometers) due to the largest expected amplitude h of a gravitational wave. Being the arm length change proportional to the arm length, it is evident that the interferometer sensitivity is determined by its dimensions. Due to several reasons, including the earth surface curvature, ground based interferometers have been designed and built with up to few kilometer arm length.

Given the extremely small signal, the main challenge for all detectors is to be protected against spurious phenomena able to produce fake signals. In particular all existing and planned interferometers^{3,4,5} have optical components suspended to sophisticated pendulum chains, to attenuate seismic vibrations; moreover almost the whole light path runs inside ultra-high-vacuum enclosures.

2 Virgo layout

In Figure 1 a simplified optical layout of the Virgo interferometer is shown. As it will be explained, Virgo is not a bare Michelson interferometer; several optical components are used in addition to the classical 50% reflecting beam splitter (BS) and 100% reflecting terminal mirrors (NE and WE). Virgo works on the “dark fringe”, that is the terminal mirror positions are set in order to have a π phase difference between the return beams, superimposing on the detection arm. In this way there is destructive interference and the detection photodiodes (B1) on the external detection bench (EB) see a null light signal, besides their own noise. At the passage of a gravitational wave the arm lengths are changed, the π phase difference is slightly modified and the photodiodes receive a tiny light signal.

In Figure 1 the optical elements are shown, together with photodiodes (labeled Bi) and quadrant split photodiodes (labeled Qi); also the light beams can be seen, including some secondary reflections, used for control purposes.

2.1 Seismic isolation and vacuum system

All the sensitive optical components are suspended to 9 m tall passive/active pendulum chains, called “Superattenuators”, able to reduce seismic noise by a factor larger than 10^{12} , above a few Hz. This feature has been designed to extend the Virgo detection range down by one decade in frequency, with respect to other existing interferometers.

In order to avoid acoustic noise and thermal exchange, Superattenuators are enclosed inside huge vacuum tanks 11 m tall and 2 m in diameter. Those vacuum tanks, together with the light path vacuum tubes (two tubes 3 km long, 1.2 m in diameter), constitute one single ultra-high-vacuum volume of about 7000 m^3 , kept below 10^{-9} mbar.

Around the interferometer there are also a few optical benches (LB, DT, EB, NEB, WEB, in Figure 1) outside the vacuum enclosure, attached to ground, accommodating optical devices not requiring seismic isolation.

2.2 The light source

The light beam entering the interferometer is produced by an injection locked master/slave laser system (Nd:YAG/Nd:YVO₄), able to deliver 20 W at $\lambda = 1064 \text{ nm}$.

After passing on the DT optical bench to be correctly aligned to the interferometer, the beam enters the vacuum system reaching the suspended input optical bench (IB). A fraction of the beam is sent to a 30 cm monolithic triangular cavity (RFC) to stabilize the laser frequency below 15 Hz. Then the beam resonates in a triangular cavity (IMC, Input Mode Cleaner), 144 m long, constituted of in vacuum suspended mirrors; the coming out beam turns out to be spatially

filtered and enters the interferometer through the power recycling mirror (PR) with a power of 10 W.

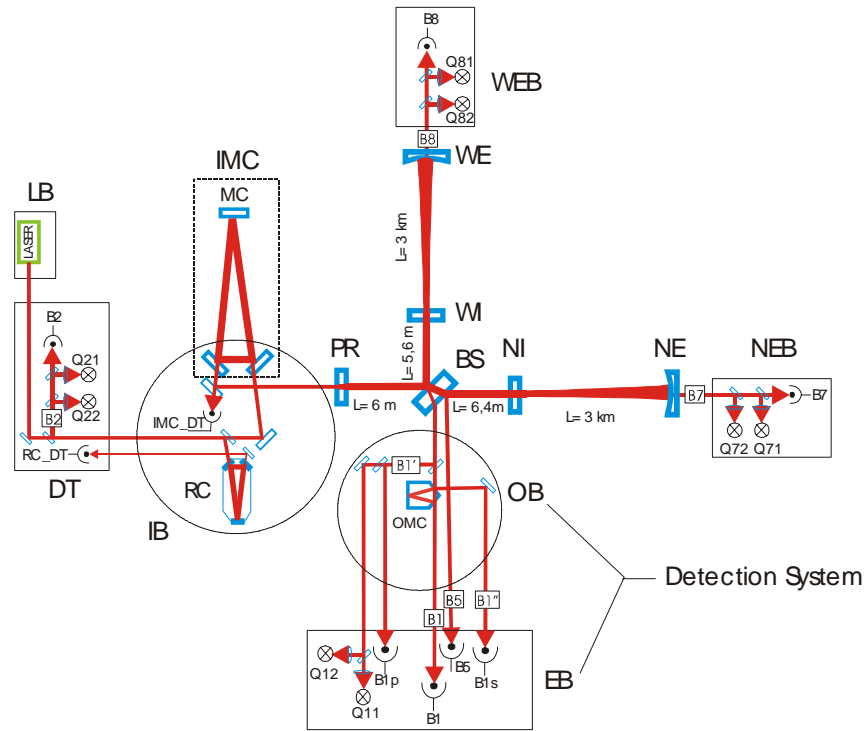


Figure 1: Interferometer optical layout

PR is a 92.5% reflecting mirror, maintained by a feedback control in a position such that all the light returning to the laser is sent back to the interferometer, perfectly in phase with the incoming light. In this way an overall resonant cavity is set up, the entrance end being constituted by the PR mirror, the other end by the whole Michelson interferometer. It has to be noticed that, with the interferometer set on the dark fringe, all the light fed-in by the laser system returns to it, apart a negligible fraction lost by absorption and scattering off the mirrors. The effect of power recycling is to multiply the light power entering the interferometer by a factor of 50, being 80 the finesse of the recycling cavity. This is equivalent to use a 0.5 kW laser, not available at present. To have 50 times more power circulating in the interferometer reduces by a factor of $\sqrt{50}$ the Shot noise, due to the statistical fluctuations of the number of photons; this noise dominates above 500 Hz.

2.3 The Michelson interferometer

At the interferometer entrance, the BS mirror splits the beam in a 90° reflected beam, sent towards the West arm, and a transmitted beam, sent towards the North arm. At 3 km distance, on each arm, there is a 100% reflecting mirror to send back the light beam. In order to enhance the phase change induced on the beams by the arm length change (due to passing gravitational waves), it is convenient to let each beam go back and forth several times along its arm, before to recombine at BS. This is most conveniently achieved introducing an 88% reflecting mirror at the entrance of each arm, so constituting two 3 km long Fabry-Perot resonant cavities, with a finesse of 50. In such a Fabry-Perot cavity the entrance mirror is flat and the terminal mirror is spherical, with a curvature radius of about 3.5 km; the beam spatial distribution is “gaussian”.

Hence photons run along the arms $2/\pi \cdot 50$ times, in average, increasing by the same factor the accumulated phase change.

It is worth to remark that, with this scheme, we have 8 kW of light power circulating in each arm. This puts very severe limits on mirror absorption, both in the substrate and on the reflecting coatings. A too high power release in the mirrors would produce a local temperature increase and an intolerable deformation of the mirror surface; this effect is largely increased by the poor heat exchange, in vacuum.

2.4 The signal detection

The output beam, possibly containing the gravitational wave signal, propagates in the direction opposite to the West arm, passing on the suspended output bench (OB) and finally reaching the external detection bench (EB). In its path the beam goes through a monolithic output mode cleaner (OMC), in order to filter out higher order modes, originated by several possible optical defects.

Many auxiliary beams are also sampled out and directed on photodiodes and quadrants for control purposes. Finally the output signal is distributed on a set of 16 high quantum efficiency InGaAs photodiodes (B1).

3 Commissioning the detector

The goal of the commissioning work is to have a detector fully operative, starting from the different component subsystems already individually working.

In 2002 the “central interferometer” has been commissioned; that is we have learned to control a short arm suspended Michelson interferometer, limited to BS, NI and WI mirrors, including the whole laser system, the detection system, data acquisition and data storage.

After completion of the arm vacuum tubes and the installation of the terminal mirrors, commissioning of the full interferometer has been started, in July 2003.

The commissioning activity has been logically divided in three steps:

- a. align and operate separately the Fabry-Perot cavities of the two arms
- b. operate together the two arms, tuning the Michelson on the dark fringe
- c. align and control the PR mirror and bring to resonance the power recycling cavity.

At the time of the conference in Hanoi (August 2004) phase b. was almost completed; in December 2004, while writing the contribution to the conference proceedings, also phase c. has been almost completed.

The commissioning work consists of setting up and learning to operate a complex control system, with the aim to keep steady at 10^{-12} m level several mirrors, 3 km apart, suspended under vacuum to pendulum chains 10 m tall. One of the largest effects to be corrected is the earth tide; this natural phenomenon changes the 3 km arm length by up to 200 μ m, with a 12 hours period.

In Figure 2 a simplified scheme of the Virgo control system is shown.

Error signals are supplied by photodiodes and quadrants as well as by accelerometers and LVDT's (linear variable differential transformers), accommodated on the different stages of the Superattenuator chains.

Correction signals are generated by a fully digital control system, totally developed and built in the various laboratories of the collaboration, both hardware and software parts.

Correction actions are performed by a large variety of actuators, including stepping motors, piezoelectric devices, Peltier cells and coil-magnet pairs.

Progress in commissioning has been made easier by the development of a complete simulation software, allowing to fully simulate the behaviour of the detector (mechanics, optics and electronics), both in time and in frequency domain.

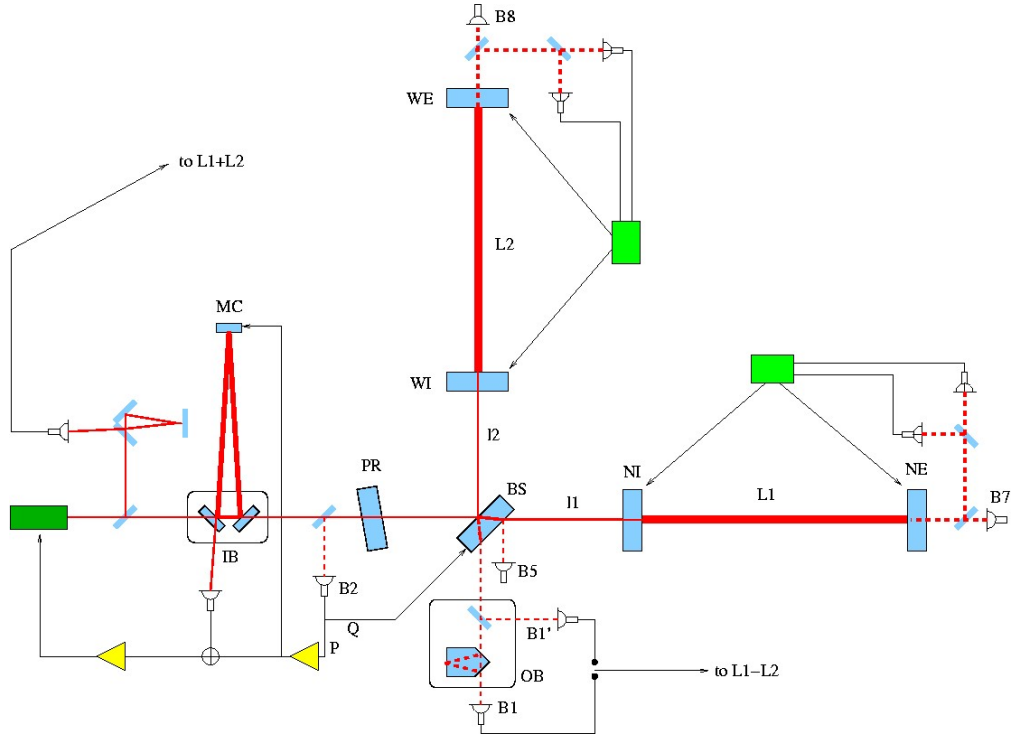


Figure 2: The interferometer control system. The thin black arrows show the signals used to control the different mirrors. The 3 km distances $L1$ and $L2$ have to be controlled to keep the arm Fabry-Perot cavities in resonance. The distances $I1$ and $I2$ have to be controlled to keep the interferometer on the dark fringe. The laser frequency stabilization is given, below 15 Hz, by the monolithic reference cavity, at higher frequencies by the long arm cavities.

While progressing in the commissioning activity, several data acquisition runs have been performed, with the aim to measure the achieved sensitivity and to test the capability to maintain the detector in stable operating conditions for several days. Six commissioning runs (C0 – C5) have been performed so far, with full 3 km long arms, with progressively more complete interferometer configuration and improving sensitivity; duty cycles (fraction of time in smooth operating conditions) ranging between 70% and 90% have been obtained.

In Figure 3 the design sensitivity is shown (lower curve), together with the C3 run sensitivity, measured in April 2004 (upper curve) and the C4 run sensitivity, measured in June 2004 (intermediate curve). Sensitivities as a function of the frequency (Hz) are shown as linear power spectra of the gravitational wave adimensional amplitude.

In December 2004, after the conference in Hanoi, a further run has been performed, working for the first time with the power recycling in operation. The sensitivity turned out to be lowered (i. e. improved) by about five times.

4 Perspectives and conclusions

At present Virgo sensitivity is higher than the design one by a large factor, in most of the frequency range. This difference is expected to be strongly reduced around mid 2005. At that moment it could be possible to take data contemporarily with the other operating interferometers, having comparable sensitivity. To this aim a robust effort has been started, to prepare common analysis strategies and software in collaboration with LIGO, the Caltech/MIT collaboration. In fact, trying to detect tiny signals superimposed on relatively large background, it is mandatory to make coincidences between totally decoupled detectors.

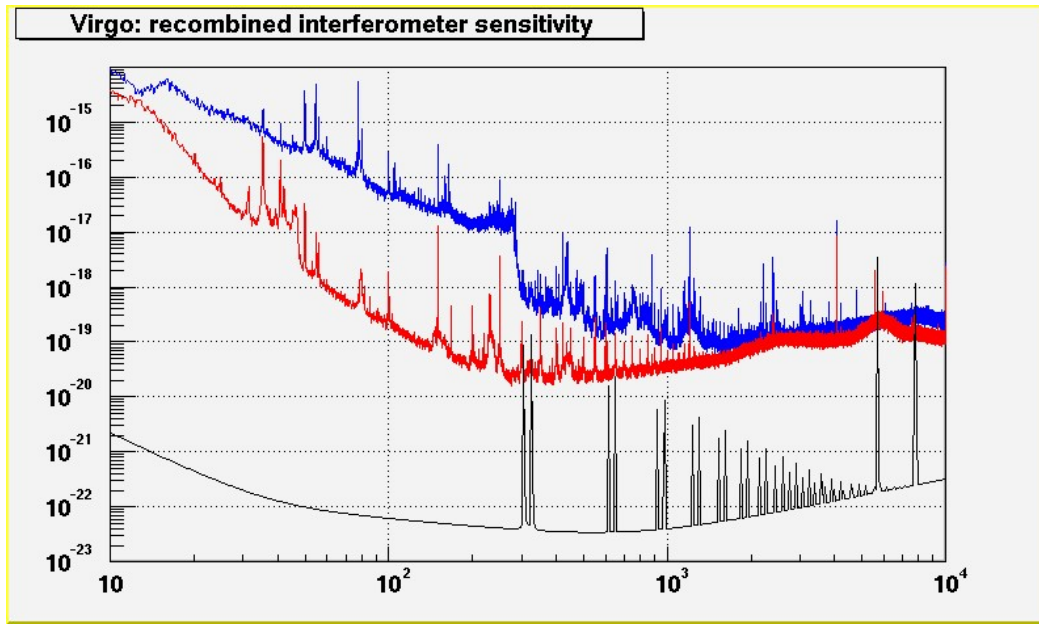


Figure 3: Virgo sensitivity in $\text{Hz}^{-1/2}$ as a function of the frequency (Hz). The lowest curve shows the design sensitivity; the intermediate curve is the measured sensitivity during the C4 run, in June 2004; the upper curve is the measured sensitivity during C3 run, in April 2004.

The announced improvement will be possible through two sets of actions:

- implementation of already planned steps of the commissioning activity
 - complete the implementation of power recycling
 - improve the laser frequency stabilization
 - improve the automatic locking acquisition
 - build new low noise DAC and coil drivers to steer the mirrors.
- improvements made necessary by unexpected problems
 - build a new suspended injection bench (IB), including a Faraday isolator to cut the light back-reflected in the MC cavity
 - replace the composite PR mirror with a monolithic one.

All these actions have already been started and most of them are quite advanced. It is expected to conclude all improvements before mid 2005.

References

1. C. Bradaschia et al., *Nucl. Instr. and Meth. A* **289**, 518-525 (1990).
2. D. Blair and Ju Li: Towards Advanced Gravitational Wave Detectors - a review of gravitational wave research around the world, *these proceedings*.
3. D. Sigg et al., *Class. Quant. Grav.* **19**(7), 1429-1435 (2002).
4. M. Ando et al., *Class. Quant. Grav.* **19**(7), 1409-1419 (2002).
5. B. Willke et al., *Class. Quant. Grav.* **19**(7), 1377-1387 (2002).